Published in final edited form as:
J Comp Neurol. 2012 June 1; 520(8): 1819–1830. doi:10.1002/cne.23015.

SECOND ORDER INPUT TO THE MEDIAL AMYGDALA FROM OLFACTORY SENSORY NEURONS EXPRESSING THE TRANSDUCTION CHANNEL TRPM5

John A. Thompson[1,2], **Ernesto Salcedo**[1,2], **Diego Restrepo**[1,2], and **Thomas E. Finger**[1,2]

[1]Rocky Mountain Taste and Smell Center, Department of Cell and Developmental Biology, University of Colorado Anschutz Medical Campus, Aurora, Colorado 80045

[2]Neuroscience Program, University of Colorado Anschutz Medical Campus, Aurora, Colorado 80045

Abstract

Recent anatomical tracing experiments in rodents have established that a subset of mitral cells in the main olfactory bulb (MOB) project directly to the medial amygdala (MeA) traditionally considered a target of the accessory olfactory bulb. Importantly, neurons that project from the MOB to the MeA also show activation in response to conspecific (opposite sex) volatile urine exposure, establishing a direct role of the MOB in semiochemical processing. In addition, olfactory sensory neurons (OSN) that express the transient receptor potential M5 (TRPM5) channel innervate a subset of glomeruli that respond to putative semiochemical stimuli. In this study, we examined whether the subset of glomeruli targeted by TRPM5 expressing OSNs are innervated by the population of mitral cells that project to the MeA. We injected the retrograde tracer cholera toxin B (CTB) into the MeA of mice in which the TRPM5 promoter drives green fluorescent protein (GFP). We found overlapping clusters of CTB-labeled mitral cell dendritic branches (CTB (+)) in TRPM5-GFP positive (TRPM5-GFP (+)) glomeruli at significantly greater frequency than expected by chance. Despite the significant degree of co-localization, some amygdalopetal mitral cells extended dendrites to non-TRPM5-GFP glomeruli and vice versa, suggesting that although significant overlapping glomerular innervation is observed between these two features, it is not absolute.

Keywords

TRPM5; medial amygdala; main olfactory bulb; semiochemical

INTRODUCTION

The vomeronasal organ (VNO) and the main olfactory epithelium (MOE) form two quasi-independent networks for transduction of odor information in the rodent olfactory system. Classical work suggested that the VNO, but not the MOE, detects chemosignals associated with social identity and behavior, including pheromones and other semiochemicals (Scalia and Winans, 1975), whereas the MOE functions in general detection of volatile compounds. However, recent evidence shows that both olfactory subsystems can detect and process socially relevant chemosignals (Restrepo et al., 2004; Lin et al., 2007; Kang et al., 2009). Indeed, genetic deletion of VNO receptors (Leypold et al., 2002; Stowers et al., 2002) and

Corresponding Author: John A. Thompson, University of Colorado Anschutz Medical Campus, Aurora, Colorado, 80045, john.a.thompson@ucdenver.edu.

VNO ablation affects many chemosignal driven behaviors (Petrulis et al., 1999; Pankevich et al., 2004), such as intruder aggression, and mounting behavior, but do not impair sex discrimination.

Within the olfactory bulb, signals from the VNO terminate in the accessory olfactory bulb (AOB), whereas the MOE transmits information to the main olfactory bulb (MOB). Higher-order connections of the MOB and AOB also tend to remain segregated (Scalia & Winans, 1975). The AOB projects predominantly to the medial amygdala (MeA), and posterior and anterior cortical amygdala (PCo, ACo; Scalia & Winans, 1975; Licht and Meredith, 1987). In contrast, the MOB projects to a distinct set of cortical regions including the anterior olfactory nucleus, piriform cortex, and cortical amygdala (Scott et al., 1980; Luskin and Price, 1983; Schoenfeld and Macrides, 1984). AOB and MOB pathways converge in several cortical and sub-cortical amygdalar targets (i.e., posterior medial cortical amygdala and medial amygdala), suggesting a location for integration of chemosignals involved in social communication.

Neural activation in MeA following semiochemical stimulation has implicated the MeA in processing volatile information from the AOB (Samuelsen and Meredith, 2009a, b). Moreover, recent studies combining anatomical tracing and cfos expression in MOB following exposure to conspecific urine shows compelling evidence for a direct pathway from MOB to MeA (Kang et al., 2009, 2011). However, identification of the subset of olfactory sensory neurons (OSN) in the MOE that subserves this specialized connection from the MOB to MeA remains unknown. The transient receptor potential channel M5 (TRPM5), a downstream target in the cAMP cascade (the canonical signaling cascade for transduction of odor stimuli), is expressed in a subset of MOE OSNs, and their glomerular targets show activation in response to putative social chemosignals (Lin et al., 2007). In this study, we sought to determine if the glomerular targets of TRPM5 expressing OSNs preferentially contact dendrites of MOB mitral cells that project to the MeA. We injected the retrograde tracer cholera toxin B (CTB) into the MeA of mice in which the TRPM5 gene drives expression of green fluorescent protein (TRPM5-GFP). This permitted assessment of whether dendrites of retrogradely labeled mitral cells were preferentially associated with glomeruli receiving input from TRPM5-expressing OSNs.

METHODS

Animals

Mice were bred in the animal facilities of the University of Colorado Anschutz Medical Campus. We used adult TRPM5-GFP mice (n = 6) of both sexes (3 males and 3 females; age, 71 – 191 days). TRPM5-GFP animals on C57BL/6J background were provided by Dr. Robert Margolskee (Monell Chem Senses Ctr., Philadelphia, PA). The TRPM5-GFP construct contains 11 kb of mouse TRPM5 5′ flanking sequence, TRPM5 Exon 1 (untranslated), Intron 1, and the untranslated part of Exon 2, and eGFP (Clapp et al., 2006). Since, these animals are transgenic both alleles of TRPM5 are intact. We used polymerase chain reaction (PCR) to genotype the offspring for the presence of GFP. The animals were housed in a vivarium with a 12 h reversed light/dark cycle with lights off at 11:00 am. Food (Teklad Global Rodent Diet #2918; Harlan) and water were available *ad libitum*. All animal procedures were performed in accordance with NIH guidelines and were approved by the Institutional Animal Care and Use Committee at the University of Colorado Anschutz Medical Campus.

Cholera toxin injection

Three males and two females received bilateral MeA injections and one female received a unilateral injection. The cholera toxin injection adheres closely to the injection protocol delineated by Cetin et al. 2006. Mice were exposed briefly to a volatile anesthesia (isoflurane; 200 μL). Immediately after the animal became anesthetized, mice were deeply anesthetized with an intraperitoneal injection of ketamine/xylxaine (100 μg/g and 20 μg/g, respectively) into the lower left abdominal quadrant. Use of the volatile anesthesia reduced stress ensuring a reliable effect of the deep anesthetic. Foot pinch was used to confirm depth of anesthesia. When the animal was fully unresponsive to foot pinch, the fur on the surface of the scalp from the midline of the orbits to ears was removed and topical antiseptic (Betadine) was applied along with ophthalmic ointment on the eyes. After the animal was secured in the stereotaxic instrument a bolus of topical anesthetic (lidocaine; 25 μl) was injected under the surface of the scalp. With the skull exposed by central incision and scalp retraction, we aligned bregma and lambda along the horizontal plane (z coordinate) and drilled small cranial apertures over the approximate location of the MeA (Caudal: −1.2 mm (relative to Bregma); Lateral: ±1.91 mm (relative to midline).

Injection pipettes were pulled from borosilicate glass micropipettes (OD: 1.0mm, ID: 0.5mm; Sutter Instruments) using a Model P97 Sutter Instrument micropipette puller and the tips were clipped under microscope inspection to 10–15 μm inner diameter using dissection scissors. The volume of the injection was calibrated by making 1 mm demarcations along the shaft of the glass pipette with a fine tipped black marker (1 mm = ~125 nl).

Two μl of cholera toxin subunit B conjugated to Alexa 555 (CTB; Invitrogen, Molecular probes, Inc.) reconstituted in 0.1 M phosphate buffered saline (PBS; pH 7.3) was pipetted onto a small square (0.5 cm x 0.5 cm) of paraffin film and placed on the surface of the skull approximately over the first craniotomy. Then the injection pipette was lowered into the CTB and under microscope inspection ~500 nl of CTB was slowly sucked up. Taking up the tracer was achieved by having the pipette connected with 35 cm of PE-160 polyethylene tubing (OD: 1.57 mm; ID: 1.14mm) to a blunted 23 gauge needle connected to a 20ml Luer Lok syringe. The CTB filled micropipette was adjusted to the appropriate injection coordinates and slowly lowered to depth (5.2mm from dura surface). A total of ~175 – 200 nl of CTB was injected into MeA. Under low magnification, in which markings on the injection pipette could be visualized, CTB was slowly injected by applying pressure with the 20ml syringe. The total desired volume per side was injected in two approximately half volume steps separated by 5 minutes. After the final injection, the surface of the skull was scrubbed with 0.1 M PBS, the scalp was sutured with veterinarian adhesive and topical anesthetic was reapplied along with a topical antibiotic (Gentamicin).

Immunocytochemistry

Strong fluorescent signals were obtained for GFP expression by immunohistochemical detection of GFP with a chicken polyclonal anti-GFP antibody (catalog#GFP-1020, lot#1223FP03, working dilution 1:3000; Aves Labs Inc.). Detection of Alexa 555 conjugated CTB was enhanced by application of rabbit anti-CTB antiserum. According to the manufacturer data sheet, the anti-GFP antibody was isolated from IgY fractions of egg yolks from GFP-immunized chickens and the specificity was verified by Western blot analysis and immunohistochemistry on tissue from transgenic GFP-expressing mice. Also, no GFP label was observed when applied to sections of olfactory bulb from wild type mice (data not shown). CTB and the anti-CTB antibody (catalog#V34404, lot#883904, working dilution 1:2000; Invitrogen Molecular Probes) were purchased as a kit (Invitrogen Molecular Probes, #V34404). Anti-CTB antibody specificity was confirmed by the absence of label when applied to olfactory bulb sections of non-injected animals (data not shown).

At the end of a 14–19 days postoperative period, mice were overdosed with an intraperitoneal injection of sodium pentobarbital (100 mg/kg), transcardially perfused with saline followed by ice-cold 4% paraformaldehyde (PFA) in 0.1 M PB. After perfusion, brains were postfixed for 3.5 hours in 4% PFA in 0.1 M PB and then cyroprotected overnight by immersion in 20% sucrose in 0.1 M PB. The olfactory bulbs and forebrains were embedded in optimal cutting temperature compound (OCT; Fisher Scientific), and frozen rapidly on dry ice. Serial coronal sections (40 μM) were cut on a cryostat and maintained in order for glomerular mapping and reconstruction of the injection site. As a control, sections of olfactory bulb from wild type animals that did not have endogenous GFP were reacted with the anti-GFP antibody and did not show any fluorescence (data not shown).

Olfactory bulb—Following three 10 min washes in 0.1 M PBS, sections were incubated in blocking solution containing 1% BSA, 2% normal goat serum, and 0.3% Triton X-100 in 0.1 M PBS for 1 h and then incubated in a cocktail mixture of rabbit anti-cholera toxin subunit b and chicken anti-GFP (for details, see antisera information) for 24–48 h. Following incubation in antisera, sections were washed three times for 10 min in 0.1 M PBS. Then sections were incubated in secondary antibodies (goat anti-rabbit Alexa 568 for cholera toxin subunit b; 1:500, goat anti-chicken Alexa 488 for GFP; 1:500) for 2 hours. After secondary antibody incubation, sections were washed three times in 0.1 M PBS, once in 0.1 M PB, mounted in serial order onto slides and coverslipped with a 1:3 ratio of Vectashield DAPI mounting medium (Vector Laboratories Inc.) to Fluormount-G (Biotech, Birmingham, AL). DAPI was used to reveal olfactory bulb cytoarchitecture.

Forebrain sections containing amygdala—Following three 10 min washes in 0.1 M PBS, sections were incubated in a 488 fluorescent Nissl stain solution (1:100; NeuroTrace, Invitrogen, catlog#: N-21480) mixed with 0.1 M PBS and 0.3% Triton X-100 for 15 minutes. Following Nissl staining, sections were washed three times in 0.1 M PBS and one final wash in 0.1 M PB. Sections were mounted onto slides and coverslipped with Fluormount-G.

Olfactory Bulb Mapping

In order to determine the extent of CTB retrograde labeling and measure the proportion of CTB colocalization with TRPM5 expression in the glomerular layer, we used GLOM•MAP (http://www.ucdenver.edu/academics/colleges/medicalschool/centers/tastesmell/Pages/software.aspx) mapping software running in MATLAB (The MathWorks, Natick, MA; Salcedo et al., 2005) to map the location of every glomerulus and a significant proportion of the CTB positive mitral cells. Bulb sections used to generate glomerular and mitral cell maps were digitally photographed to create a montage at 10x using Q Capture software (QImaging) with a monochrome Q-imaging camera on an Olympus BX41TF microscope. Image capture settings were set using three randomly selected bulb sections on the slide to minimize saturated pixels and those settings (exposure time and gain) were consistently applied to every section within the case to normalize intensity values across sections. Overlapping images of individual bulb sections were imported into Adobe Photoshop (CS4) and merged into a single contiguous image using the photomerge tool. We mapped every other section so that spacing between mapped sections was 80 μm along the rostrocaudal axis. Within GLOM•MAP, on each section we segmented the boundary between the glomerular layer and the external plexiform layer with a traced perimeter line. To establish a coordinate axis for each stamped glomerulus, we manually aligned an orientation line parallel to the dorsoventral axis of the bulb section from the dorsal peak of the mitral cell layer to the base of mitral cell layer. Once aligned, the angular coordinates of each

glomerulus were recalculated so that 0°, 90°, 180°, and 270° correspond to the dorsal, lateral, ventral, and medial surfaces of the MOB, respectively.

Mapping of Injection

To estimate the extent of the CTB injection in MeA, photographs of serial sections representing MeA were captured at 4x using the same microscope and camera equipment as used for olfactory bulb imaging. Images of serial sections were imported into ImageJ in order to calculate the area and volume of MeA (visualized with 488 Nissl) and CTB injection (visualized with 555 Alexa conjugation). Within ImageJ (version 1.62 software; National Institutes of Health, Bethesda, MD), regions of interest could be defined easily and traced for both CTB injection area and the nuclear boundaries of Nissl defined MeA. To derive the percentage of MeA covered by each injection, the area of Nissl defined MeA and the area of CTB within the boundary of MeA was traced and calculated for each section.

Analysis

Identification of Glomeruli—In each bulb section, we traced every glomerulus and the position of CTB (+) mitral cells using a glomerular tracing tool in GLOM•MAP. The GLOM•MAP software allowed visual inspection of the image of the bulb in all three RGB channels both independently and merged. The following steps were taken to identify different populations of labeled glomeruli in each section. First, the green channel was selected and TRPM5-GFP (+) glomeruli were identified and traced. Glomeruli were identified as GFP-positive if the green intensity was significantly brighter than the background, as judged by the observer. GFP positive expression in the glomerular layer typically filled an entire glomerulus. Second, the red channel was selected and CTB(+) glomeruli and CTB(+) mitral cells were identified. CTB positive mitral cells were counted if the red intensity was significantly brighter than background as judged by observer. Combination of the conjugated Alexa 555 fluorophore with a CTB antibody reaction clearly differentiated CTB labeled mitral cells from background and unlabeled mitral cells. CTB(+) glomeruli were traced and counted if CTB positive dendritic processes were observed within the glomerular boundary. Glomeruli were identified as CTB(+) if any CTB positive mitral processes were identified within their boundaries. Third, previously traced GFP(+) and CTB(+) tags were superimposed, and overlapping tags were designated CTB(+) and TRPM5(+). Finally, the blue channel (DAPI stain) was selected and all remaining glomerular boundaries that did not have labeled tags were traced and counted as unlabeled glomeruli.

Calculating proportion—To measure the extent of CTB(+) expression in the glomerular layer and determine whether colocalization with MeA projections occurred in TRPM5-GFP(+) glomeruli we used the glomerular boundary tags identified in GLOM•MAP. From these identified glomeruli, we calculated the proportion of unlabeled glomeruli, TRPM5-GFP (+) only glomeruli, CTB(+) only glomeruli, and TRPM5-GFP & CTB (+) glomeruli across the entire the bulb. Across 6 bulbs, a total of 247 bulb sections were imaged and mapped (45.7 ± 5.5; mean ± SD; range 36 – 51), and a total of 16,746 glomeruli were traced and mapped (2971 ± 287.2; mean ± SD; range 2282 – 3057 per unilateral bulb).

Anatomical localization of each glomerulus was determined for both the rostral/caudal axis and the dorsal/ventral axis. To obtain the approximate dorsal/ventral location GLOM•MAP applied an angle value (i.e., 90° = medial) using the coordinate axis for each stamped glomerulus when aligned to the orientation line drawn down the center of the bulb section. The rostral/caudal location was extracted by multiplying bulb section distance with bulb section number. That is, a glomerulus mapped in the 4^{th} section would be designated with a rostral/caudal value of 240 μm (80 μm x 4). From this information a density histogram was

generated to reflect the spatial distribution of each glomerular population by plotting the dorsal/ventral position (dorsal-ventral-dorsal angle) on the y axis and rostral/caudal position (distance) on the x axis and density of glomeruli on the z axis.

Pixel Intensity measurement—Pixel intensity values for each RGB channel were calculated within every traced boundary using GLOM•MAP. To verify the difference in expression levels between TrpM5-GFP(+) glomeruli and non-TrpM5-GFP(+) glomeruli we measured the mean green pixel intensity across the pixel population within each glomerular boundary for both populations and calculated the distance between those two distributions.

As CTB labeling in the glomerular layer reflected dendritic terminations from the mitral cell layer, the bright pixels were scattered across glomeruli in most cases. To measure the difference between CTB(+) and non-CTB(+) glomeruli and take into account the sparse labeling of CTB within the glomerulus we calculated the ratio of pixel intensity values based on a stringent threshold (mean + 2 standard deviations). In GLOM•MAP, within each section, we randomly selected four traced CTB(+) glomerular boundaries and calculated the distribution of red (CTB) pixel intensity values. Using this distribution, we extracted the threshold (mean + 2 standard deviations) and applied that threshold to the remaining glomerular boundaries within the section. That is, for each glomerular boundary, within each bulb section, the percent of red (CTB) pixel intensity values that exceeded the derived threshold was calculated and encoded in a data sheet. Thus, for each glomerular population we derived a distribution of suprathreshold CTB(+) pixel values. We used these distributions to compare the difference in CTB(+) pixel density across glomeruli populations (TRPM5(+), CTB(+), CTB&TRPM5(+)). To determine statistically if distributions of CTB(+) pixel densities from different glomerular populations actually reflected unique distributions we used a traditional method for comparing two dimensional distributions: the KS statistic.

Confocal Imaging

For purposes of visualization, but not quantification, confocal images were captured using a Kalman filter and an Olympus Fluoview confocal laser scanning microscope (LSCM) FV300 (Olympus Corporation). For each confocal image we used a sequential channel scan which collected each channel separately. Within the Fluoview software, we applied a non-linear gamma filter to enhance visualization. Brightness and contrast were in Adobe Photoshop CS4.

Statistics

Statistical analysis was performed with Prism 4.0 (GraphPad Software Inc., San Diego, CA), and R (an open source programming environment for statistical computing; www.r-project.org). Colocalization proportion comparisons within both the TRPM5-GFP(+) and CTB(+) populations were analyzed with rank-sum tests (Wilcoxon matched-pairs signed rank tests). Pixel intensity values were treated as continuous distributions and we tested the difference between the distribution of green intensity values TRPM5-GFP(+) and the distribution of non-TRPM5-GFP(+) populations with the nonparametric Kolmogorov-Smirnov test. The difference between distributions of suprathreshold red pixels for each glomerular population was compared using the nonparametric Kolmogorov-Smirnov test. Chi-squared analysis was used to determine the strength of the correlation between TRPM5-GFP(+) and CTB(+) colocalization in the ventral region of the bulb.

RESULTS

Retrograde Injections into the Medial Amygdala

Manual pressure injections of the retrograde tracer CTB were successfully placed into MeA in 6 out of 11 injections, and these produced successful labeling in the mitral cell and glomerular layer of the main olfactory bulb. Out of the six animals, one male (5218) and one female (5289) had successfully targeted bilateral injections, two females (P5244; left hemisphere, P5226; right hemisphere) had successful unilateral injections and two males had missed injections. The disproportionate distribution of successful injections between the male and female animals did not provide sufficient data to assess the possibility of sex differences in the colocalization of CTB and TRPM5. Kang et al., 2011 show that the general localization of the small population of MOB mitral cells that project to MeA between the two sexes is similar; however, they found statistical evidence for a sex difference in the percentage of CTB positive cells in the anterior and posterior medial segments of the MOB: females had higher label in the anterior segment, whereas males had higher label in the posterior segment. The lack of a sufficient sample of successfully injected male animals in our data does not allow an analysis of between sex differences to test for this observation. Figure 1A depicts coronal serial sections through an example of a successful injection and a missed injection. As exemplified in the case depicted on the right in Fig. 1A, missed injections were largely biased dorsal and medial to MeA. For successful injections, the average percent volume of injection encompassing MeA was 39% (range 21% – 71%). Figure 1B shows an overlay within MeA of the mid-point of the injection site for each successful case (case 5218L is represented in the example injection in Fig. 2A). In Figure 1C, examination of the rostral-caudal extent of the injection for each case shows most injections (4 of 6) consistently encompassed the same area throughout MeA, whereas the others encompassed more area of the ventral region than the rostral region of MeA. Low variation in the number of CTB(+) labeled mitral cells and glomeruli were observed across injection volumes (mitral cells: 2330.3 ± 210.12; percent of glomeruli labeled with CTB: 24% ± 3%; mean ± SEM).

Distribution and extent of Retrograde MeA injection within the Mitral cell layer of the MOB

To characterize retrogradely labeled projection neurons within the MOB following CTB injection into the MeA we marked CTB(+) mitral cells in the GLOM•MAP program. Figure 2A shows a density scatter plot of the spatial distribution of CTB(+) mitral cells using the rostral/caudal and dorsal/ventral location encoded on the CTB(+) mitral cell tags during the mapping process in GLOM•MAP. Along the x and y axes of the density scatter plot, histograms are used to emphasize the frequency of expression for the respective dimension, notably the dorsal/ventral angle axis shows a peak in frequency in the ventral portion of the distribution. Similar to previous work from Kang et al., (2009), we found that retrogradely labeled mitral cells from MeA concentrated largely within the ventral region of the MOB. Figure 2B summarizes the spatial distribution of CTB(+) mitral cells across cases by collapsing the rostral/caudal data and representing the dorsal/ventral angle frequency of mitral cell labeling as a polar coordinate plot. This plot highlights the low variability across cases in the location of CTB(+) mitral cells.

Figure 2C, shows two representative bulb sections from different cases of successful MeA injections in which CTB-labeled mitral cells are observed around the circumference of the mitral cell layer. Although, CTB(+) mitral cells occur in all quadrants of the bulb, the high density in the ventral region corresponds in the mitral cell layer to the general region receiving input from TrpM5-expressing receptor neurons.

In order to map which glomeruli contained dendrites of the CTB(+) mitral cells, we mapped the location of all glomeruli containing CTB(+) retrogradely labeled processes. The extent of the labeled dendritic processes varied across glomeruli. Figure 3 illustrates the variability in morphology of mitral cell terminations which varied from a single dendrite to extensive arborization. In many cases, only sinuous or globular ends of retrogradely labeled dendrite branches were evident (see Figure 3B and C; Figure 3D depicts glomerulus with no CTB label).

Mitral cells from a Subset of Glomeruli Targeted by TRPM5-GFP Expressing OSNs Send Axons to MeA

In TRPM5-GFP mice successfully injected by CTX in MeA, surveys of the olfactory bulb revealed that a subset of TRPM5-positive glomeruli contained dendrites of mitral cells retrogradely labeled from the MeA (Fig. 3, 4). Figure 4 shows images of sections from two successful MeA injections illustrating examples of co-localization and non-co-localization of primary dendrites from mitral cells labeled by cholera toxin (CTB(+), purple) and glomerular innervation from axons from OSNs that express GFP driven by the TRPM5 promoter (TRPM5-GFP(+), green). In the left panel (A) two examples of glomeruli that are only CTB(+) have been encircled by dashed lines. In the right panel (B) dashed circles highlight two TRPM5-GFP(+) glomeruli that co-localize with extensive CTB(+) mitral cell terminations.

Pixel Intensity Measure

Comparison of TRPM5-GFP intensity across cases between TRPM5-GFP(+) identified glomeruli and GFP-negative glomeruli TRPM5-GFP(−) with a nonparametric comparison revealed that they were significantly distinct distributions (KS statistic: 0.56, p value = 2.2e-16).

For CTB label, comparisons of distributions of pixel density values from the three glomerular groups (TRPM5-GFP(+), CTB(+), and TRPM5-GFP(+) & CTB(+)) revealed that CTB(+) pixel densities for both CTB(+) and TRPM5-GFP(+) & CTB(+) populations were significantly higher than for TRPM5-GFP(+) (KS statistic = 0.185, $p < 0.001$; KS statistic = 0.14, $p < 0.05$, respectively). This indicates that the distributions of CTB(+) pixel densities within both CTB(+) and TRPM5-GFP(+)&CTB(+) glomeruli were higher than within the TRPM5-GFP(+) glomeruli. However, CTB(+) pixel densities for both CTB(+) and TRPM5-GFP(+) & CTB(+) were not significantly distinct populations (KS statistic = 0.093, $p = 0.24$) indicating that glomeruli within those populations had equivalent CTB(+) pixel densities.

Extent and Identity of Retrogradely labeled Glomeruli

Figures 5A and C show the spatial distribution in the glomerular layer of CTB(+) and CTB(+) & TRPM5-GFP(+) identified glomeruli using density scatter plots. Along the rostral/caudal and angular axes of the density scatter plots we plotted a frequency histogram for each dimension to emphasize areas of peak labeling. Consistent with previous reports localizing MeA-projecting mitral cells in the ventral portion of the MOB we found a concentration of glomeruli with CTB(+) mitral terminations in the ventral area (Kang et al., 2009, 2011; see Figure 5A). Also, similar to Lin et al., 2007, we found that glomeruli targeted by TRPM5-GFP(+) OSNs show a high density in the ventral region of the bulb. Thus, in this ventral region numerous glomeruli contained both TRPM5-GFP axon arbors and CTB labeled dendrites (see Figure 5C). Both CTB(+) single-label and CTB(+)/TRPM5-GFP(+) double-label populations show a relatively uniform distribution in the rostral/caudal axis. Polar plots in Figures 5B and D show density data collapsed across the anterior/

posterior axis to highlight the low variability across cases and consistency in the increased ventral concentration of these glomerular populations.

To determine the proportion of CTB(+) glomeruli that colocalized with TRPM5-GFP(+) glomeruli, we calculated the proportion of each separate population as a percent of the entire glomerular population and the CTB(+)/TRPM5-GFP(+) as a percent of both the CTB (+) and TRPM5-GFP(+) populations. CTB(+) glomeruli comprise 24%, whereas TRPM5-GFP(+) glomeruli comprise 32% of the total population. If these markers were distributed randomly, then 8% (24% x 32%) of all glomeruli should exhibit double label. We observed that 13% of glomeruli exhibited both CTB(+) and TRPM5(+). A chi-square analysis revealed that these populations are not randomly distributed, but in fact are strongly correlated (Chi-squared = 198.93, df = 1, p =2.2e-16). Within the TRPM5-GFP(+) population, CTB(+) was colocalized in 40% of the glomeruli (Fig. 6). Conversely, within the CTB(+) population, TRPM5(+) colocalized in 52% of the glomeruli. Proportions of colocalized populations were significantly greater than their respective proportion of the entire glomerular population: TRPM5-GFP(+) (Wilcoxon, $p < 0.05$), CTB(+) ($p < 0.05$). To account for the possibility that these markers may preferentially co-localize in the ventral region of the bulb we constrained the analysis to only glomeruli in the ventral half of the bulb. A chi-square analysis revealed that co-localization between CTB(+) and TRPM5(+) in the ventral region of the bulb was similar to the entire bulb (Chi-squared = 133.9, df = 1, p=2.2e-16). These findings demonstrate that the two markers co-localize at a greater than chance level, but are not tightly correlated.

DISCUSSION

We report here that a substantial subset of glomeruli whose mitral cell population projects to the MeA receives input from TRPM5-expressing OSNs. Classical understanding of olfactory processing asserts that there are two distinct pathways for transmission of olfactory information: main olfactory system and accessory/vomeronasal olfactory system. These two pathways were thought to detect unique classes of odorant signals and terminate in different cortical regions (Winans and Scalia, 1970; Scalia and Winans, 1975). Specifically, socially relevant chemosignals were thought to be carried exclusively by the AOB, which predominantly terminates in regions of the MeA. However recent work suggests that both systems process semiochemicals and both systems converge in regions of the medial amygdala (Pro-Sistiaga et al., 2007; Kang et al., 2009, 2011). Thus, current consensus indicates that a subset of MOE mitral cells relay semiochemical signals and that the MOB transmits semiochemical information to regions of the amygdala that receives input from the AOB.

Recent work shows that pheromones, and other socially relevant chemosignals can activate TRPM5-expressing OSNs (Lin et al. 2007) and that these OSNs target glomeruli in the ventral portion of the bulb known to be activated by putative pheromones (Lin et al., 2004; Xu et al., 2005). Here we show that, while a significant portion of mitral cells innervating TRPM5-positive glomeruli innervates MeA, a subset of mitral cells innervating non-TRPM5-GFP glomeruli also projects to MeA. It is unknown whether the non-TRPM5 expressing OSN glomeruli whose mitral cells innervate MeA also respond to semiochemicals. Conversely, it remains to be determined whether the subset of glomeruli that receive input from TRPM5-expressing OSNs also respond to general odorants. Is the expression of TRPM5 in a subset of OSNs specifically linked to a subset of OSNs that respond to particular odors, or are there situations where the number of OSNs expressing TRPM5 increases and is not directly linked to expression of particular olfactory receptors? Our findings raise these as questions to be addressed in future studies.

Evidence shows that OSNs expressing TRPM5 innervate a subset of glomeruli which respond to semiochemicals such as 2,5-dimethylpyrazine and the social attractant (methylthio)methanethiol (Lin et al. 2007). Interestingly, a direct connection between the MOB and the MeA was demonstrated recently (Pro-Sistiaga et al. 2007; Kang et al., 2009, 2011). Kang and co-workers suggested that there could be a direct connection between the subset of glomeruli innervated by TRPM5 OSNs and MeA, given that these glomeruli respond to semiochemicals. Here we tested this hypothesis by identifying GFP-labeled glomeruli in TRPM5-GFP mice and surveying for co-localization with primary dendrites of mitral cells labeled from the MeA by cholera toxin. We found a significant overlap/co-localization between glomeruli that receive input from TRPM5-GFP expressing OSNs with glomeruli innervated by mitral cells projecting directly to the MeA. In addition, we confirmed previous reports that demonstrate that these MeA-projecting MOB mitral cells concentrate around the ventral portion of the MOB (Kang et al., 2009, 2011). Importantly, while a large percent of the mitral cells innervating MeA extended primary dendrites to TRPM5-labeled glomeruli, we find that mitral cells innervating the MeA do not exclusively innervateTRPM5-labeled glomeruli. Overall, these findings suggest that these two markers (TRPM5-GFP and MeA-CTB) are not randomly associated in the glomerular layer, but are strongly correlated and that glomeruli that receive input from TRPM5 expressing OSNs identify a subset of glomeruli that tend to contact MeA projecting mitral cells in the MOB.

A question arises. If the difference between the vomeronasal and main olfactory systems is not that the former deals with semiochemical signaling and the latter deals exclusively with general odorants why do two different systems exist? Clearly the AOB predominantly terminates in the MeA, and this makes sense because the AOB is predominantly involved in sensing semiochemicals. However a small fraction of MOS mitral cells that detect semiochemicals also innervate the MeA. Why is the MOB also involved in input to MeA and what does its involvement contribute to semiochemical sensing? An interesting clear difference between these two systems is that in the AOB the primary dendrite has different branches innervating multiple glomeruli (hard-wired multiglomerular processing) while in the MOB each mitral cell innervates only one glomerulus. By not hard wiring multiple glomeruli together, stimulus process in the MOB can be more flexible and in fact has been shown to change in situations where the meaning of the odor changes through learning. In these cases, interactive changes in the interneuron circuit (periglomerular interneurons and granule cells) directly modifies mitral cell output from different glomeruli (Wachowiak and Shipley, 2006; Schoppa, 2006; Doucette et al, 2011; Doucette et al, 2007; Fletcher and Wilson, 2003). Perhaps these dual systems differ on the malleability of the input, with the AOB responsible for processing hard-wired signals not easily modified and the MOB processing signals whose meanings are often altered by external behavioral input. Such an arrangement would then raise the question whether there are a subset of multiglomerular inputs to MeA that are provided by MOB mitral cells that have the ability to change multiglomerular processing based on changes in the external situations. This needs to be tested in future experiments.

Acknowledgments

We thank two anonymous reviewers for helpful feedback. This work was supported by National Institutes of Health Grants DC004657 & DC006070 to (T.F. & D.R.).

References

Cetin A, Komai S, Eliava M, Seeburg PH, Osten P. Stereotaxic gene delivery in the rodent brain. Nat Protoc. 2006; 6:3166–73. [PubMed: 17406580]

Clapp TR, Medler KF, Damak S, Margolskee RF, Kinnamon SC. Mouse taste cells with G protein-coupled taste receptors lack voltage-gated calcium channels and SNAP-25. BMC Biol. 2006; 4:7. [PubMed: 16573824]

Doucette W, Milder J, Restrepo D. Adrenergic modulation of olfactory bulb circuity affects odor discrimination. Learn Mem. 2007; 14:539–47. [PubMed: 17686948]

Doucette W, Gire DH, Whitesell J, Carmean V, Lucero MT, Restrepo D. Associative cortex features in the first olfactory brain relay station. Neuron. 2011; 69:1176–87. [PubMed: 21435561]

Dulac C, Torello AT. Molecular detection of pheromone signals in mammals: from genes to behavior. Nat Rev Neurosci. 2003; 7:551–62. [PubMed: 12838330]

Elsaesser R, Montani G, Tirindelli R, Paysan J. Phosphatidyl-inositide signalling proteins in a novel class of sensory cells in the mammalian olfactory epithelium. Eur J Neurosci. 2005; 10:2692–700. [PubMed: 15926917]

Fletcher ML, Wilson DA. Olfactory bulb mitral tufted cell plasticity: odorant specific tuning reflects previous odorant exposure. J Neurosci. 2003; 23:6946–55. [PubMed: 12890789]

Kang N, Baum MJ, Cherry JA. A direct main olfactory bulb projection to the 'vomeronasal' amygdala in female mice selectively responds to volatile pheromones from males. Eur J Neurosci. 2009; 3:624–34. [PubMed: 19187265]

Kang N, McCarthy EA, Cherry JA, Baum MJ. A sex comparison of the anatomy and function of the main olfactory bulb-medial amygdala projection in mice. Neuroscience. 2011; 172:196–204. [PubMed: 21070839]

Leypold GB, Yu CR, Leinders-Zufall T, Kim MM, Zufall F, Axel R. Altered sexual and social behaviors in trp2 mutant mice. Proc Natl Acad Sci USA. 2002; 9:6376–81. [PubMed: 11972034]

Licht G, Meredith M. Convergence of main and accessory olfactory pathways onto single neurons in the hamster amygdala. Exp Brain Res. 1987; 1:7–18. [PubMed: 3325300]

Lin W, Arellano J, Slotnick B, Restrepo D. Odors detected by mice deficient in cyclic nucleotide-gated channel subunit A2 stimulate the main olfactory system. J Neurosci. 2004; 14:3703–10. [PubMed: 15071119]

Lin W, Margolskee R, Donnert G, Hell SW, Restrepo D. Olfactory neurons expressing transient receptor potential channel M5 (TRPM5) are involved in sensing semiochemicals. Proc Natl Acad Sci USA. 2007; 7:2471–6. [PubMed: 17267604]

Luskin MB, Price JL. The topographic organization of associational fibers of the olfactory system in rat, including centrifugal fibers to the olfactory bulb. J Comp Neurol. 1983; 3:264–91. [PubMed: 6306065]

Pankevich DE, Baum MJ, Cherry JA. Olfactory sex discrimination persists, whereas the preference for urinary odorants from estrous females disappears in male mice after vomeronasal organ removal. J Neurosci. 2004; 42:9451–7. [PubMed: 15496681]

Petrulis A, Peng M, Johnston RE. Effects of vomeronasal organ removal on individual odor discrimination, sex-odor preference, and scent marking by female hamsters. Physiol Behav. 1999; 1:73–83. [PubMed: 10222476]

Pro-Sistiaga P, Mohedano-Moriano A, Ubeda-Banon I, Del Mar Arroyo-Jimenez M, Marcos P, Artacho-Perula E, Crespo C, Insausti R, Martinez-Marcos A. Convergence of olfactory and vomeronasal projections in the rat basal telencephalon. J Comp Neurol. 2007; 4:346, 62. [PubMed: 17663431]

Restrepo D, Arellano J, Oliva AM, Schaefer ML, Lin W. Emerging views on the distinct but related roles of the main and accessory olfactory systems in responsiveness to chemosensory signals in mice. Horm Behav. 2004; 3:247–56. [PubMed: 15325226]

Salcedo E, Zhang C, Kronberg E, Restrepo D. Analysis of training-induced changes in ethyl acetate odor maps using a new computational tool to map the glomerular layer of the olfactory bulb. Chem Sense. 2005; 7:615–26.

Samuelsen CL, Meredith M. Categorization of biologically relevant chemical signals in the medial amygdala. Brain Re. 2009; 1263:33–42.

Samuelsen CL, Meredith M. The vomeronasal organ is required for the male mouse medial amygdala response to chemical-communication signals, as assessed by immediate early gene expression. Neuroscience. 2009; 4:1468–76. [PubMed: 19778594]

Scalia F, Winans SS. The differential projections of the olfactory bulb and accessory olfactory bulb in mammals. J Comp Neurol. 1975; 1:31–55. [PubMed: 1133226]

Schoenfeld TA, Macrides F. Topographic organization of connections between the main olfactory bulb and pars externa of the anterior olfactory nucleus in the hamster. J Comp Neurol. 1984; 1:121–35. [PubMed: 6470206]

Schoppa NE. Synchronization of olfactory bulb mitral cells by precisely timed inhibitory inputs. Neuron. 2006; 49:271–83. [PubMed: 16423700]

Scott JW, McBride RL, Schneider SP. The organization of projections from the olfactory bulb to the piriform cortex and olfactory tubercle in the rat. J Comp Neuol. 1980; 3:519–34.

Stowers L, Holy TE, Meister M, Dulac C, Koentges G. Loss of sex discrimination and male-male aggression in mice deficient for TRP2. Science. 2002; 5559:1493–500. [PubMed: 11823606]

Wachowiak M, Shipley MT. Coding and synaptic processing of sensory information in the glomerular layer of the olfactory bulb. Semin Cell Dev Biol. 2006; 17:411–23. [PubMed: 16765614]

Winans SS, Scalia F. Amygdaloid nucleus: new afferent input from the vomeronasal organ. Science. 1970; 955:330–2. [PubMed: 5460037]

Xu F, Schaefer M, Kida I, Schafer J, Liu N, Rothman DL, Hyder F, Restrepo D, Shepherd GM. Simultaneous activation of mouse main and accessory olfactory bulbs by odors or pheromones. J Comp Neurol. 2005; 4:491–500. [PubMed: 16025460]

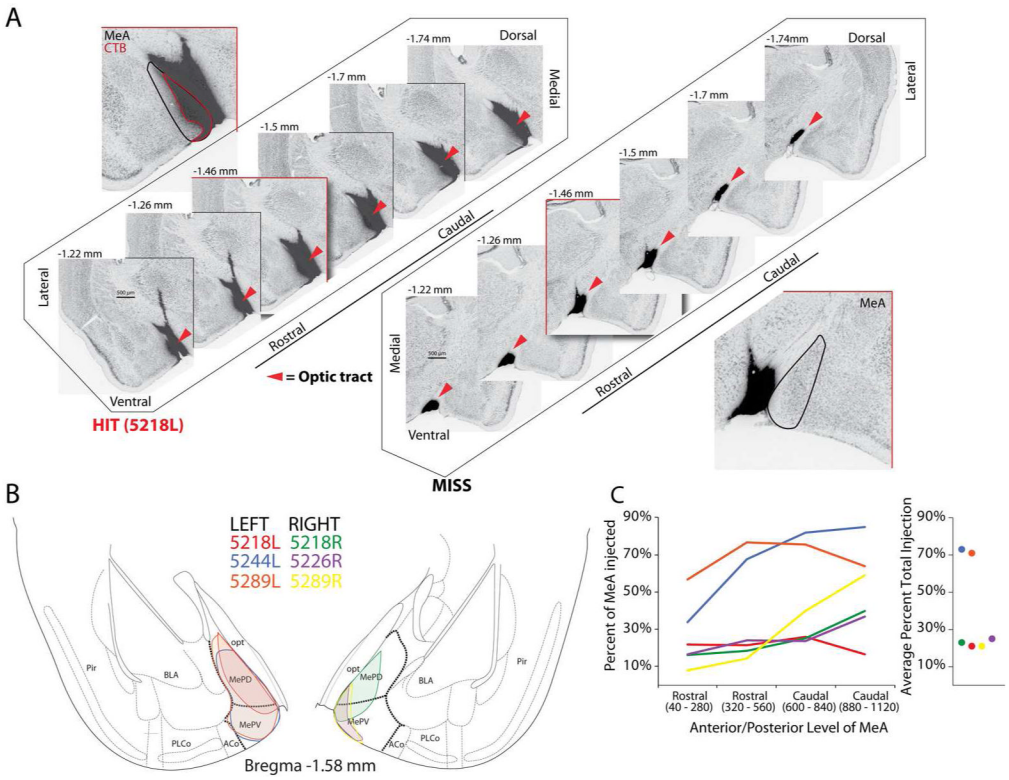

Figure 1.

Cholera toxin subunit B (CTB) injections into medial amygdala (MeA). **A.** Left series of images show representative injection into the MeA (HIT), and right series of images show representative missed injection aimed at MeA (MISS, dark label reflects CTB-conjugated Alexa 555); cytoarchitecture labeled with fluorescent Nissl (488) and fluorescent labels have been inverted and gray-scaled. Red outlined box is an enlarged representative image of injection. **B.** Overlay of region of largest cross-sectional extent of CTB label in each case in which MeA was successfully targeted (colors indicate individual successful injections). **C.** Average total volume of MeA encompassed by CTB injection and rostrocaudal distribution of CTB spread across MeA for each case. Abbreviations: Pir Piriform cortex, BLA Basal lateral amygdala, PLCo Posterolateral cortical amygdaloid area, ACo Anterior cortical amygdaloid area, MePV Medial amygdala posteroventral part, MePD Medial amygdala posterodorsal part, opt optic tract.

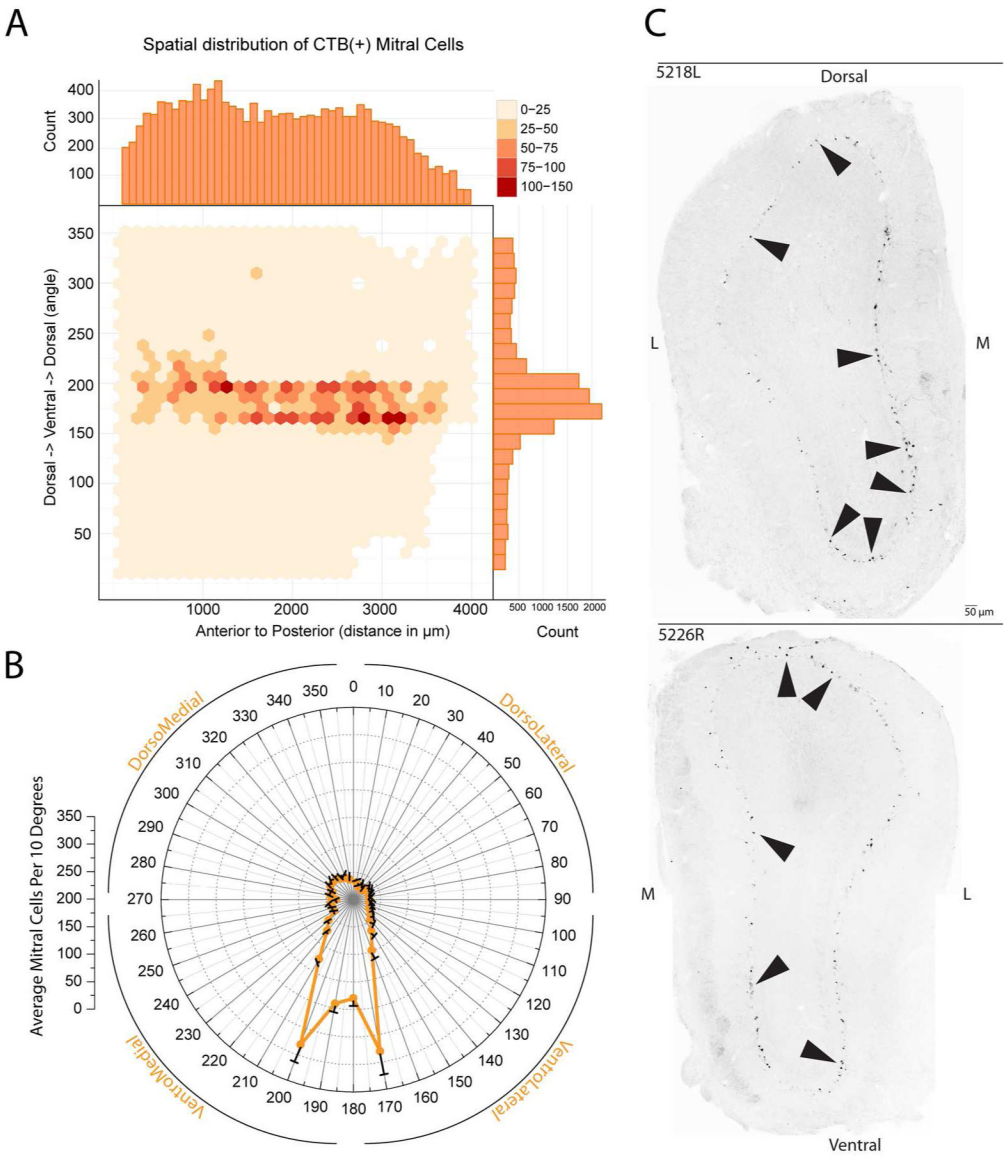

Figure 2.

Mapping of retrogradely labeled CTB(+) mitral cells in the main olfactory bulb following CTB injections in the medial amygdala. **A.** Mapping of the spatial distribution and density of CTB(+) mitral cells for the dorsoventral and rostrocaudal axes across all cases as plotted onto an unfolded map of the mitral cell layer of the olfactory bulb. The anterior-posterior axis is represented left to right (respectively) while the radial angle around the bulb is plotted on the y-axis; axis with ventral indicated by 180°. The density of labeled mitral cells (in # of cells per 30 by 30 bin) is given by the intensity of the color. **B.** Distribution of CTB(+) mitral cells across the dorsoventral axis for all cases with mean and SEM. **C.** Negative images of fluorescent (CTB-conjugated Alexa 555) micrographs of transverse sections through the olfactory bulb in two cases with successful injections into MeA. Black arrows indicate retrogradely labeled mitral cells.

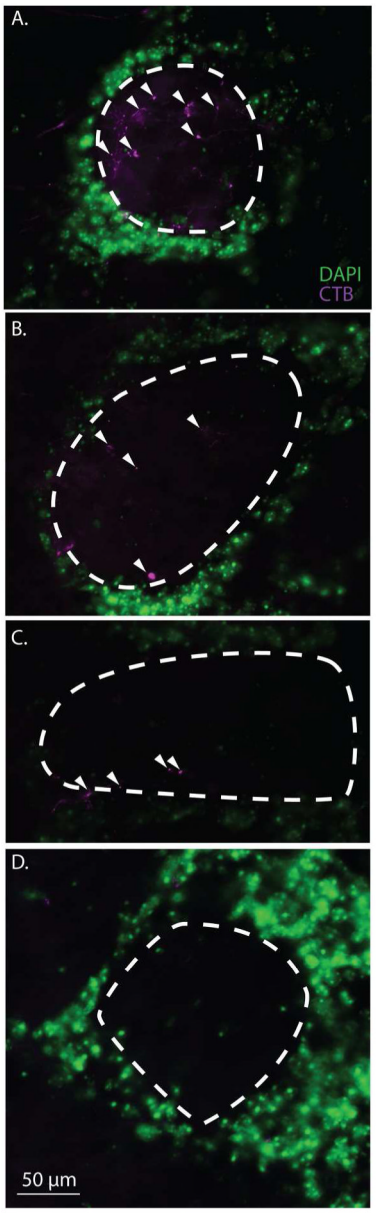

Figure 3.
Morphological features of CTB labeled mitral cell terminations within the glomerular layer. **A, B, C** show the high morphological variation in mitral cell processes labeled with CTB within the glomerular boundary following MeA injection. White arrows indicate positive CTB labeled mitral cell terminations and the white dotted line demarcates the glomerular boundary. **D.** A representative glomerulus that lacks CTB labeling.

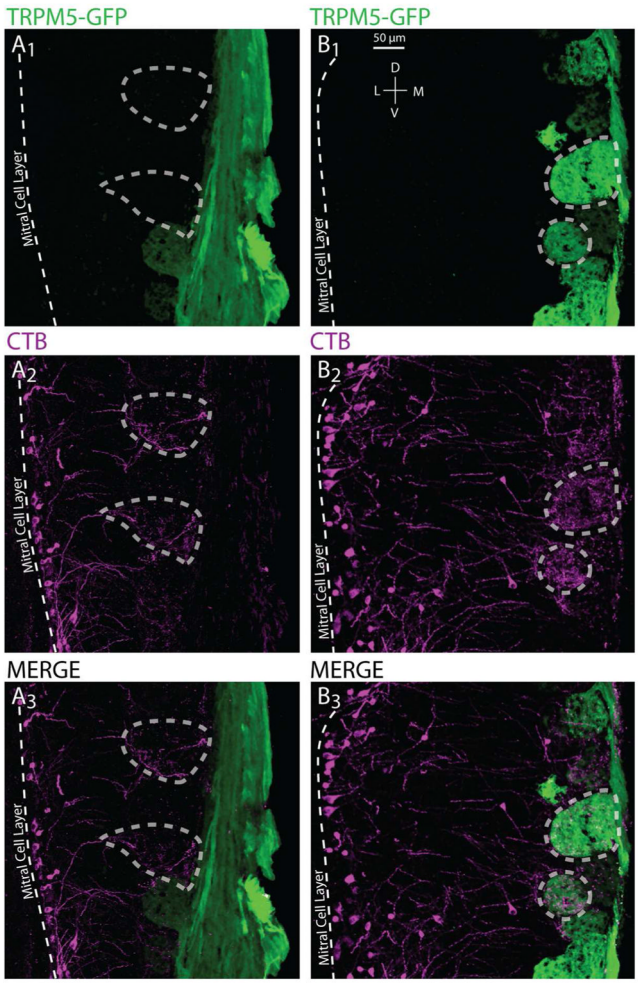

Figure 4.

Confocal images of CTB(+), TRPM5(+) and CTB(+) & TRPM5(+) glomeruli in the MOB. Sections are oriented in the coronal plane. **A** and **B** represent example regions of the MOB from two different successfully injected cases with TRPM5-GFP(+) glomeruli in green and CTB(+) mitral cells terminating in the glomerular layer in magenta. $\mathbf{A}_{1–3}$ show an example in which the TRPM5-GFP(+) expression and CTB(+) label do not overlap; dashed polygons encircle glomeruli that are labeled with CTB(+) only. $\mathbf{B}_{1–3}$ highlight examples of TRPM5-GFP(+) expression and CTB(+) label overlap in the glomerular layer; dashed polygons encircle glomeruli that express CTB(+) & TRPM5-GFP(+).

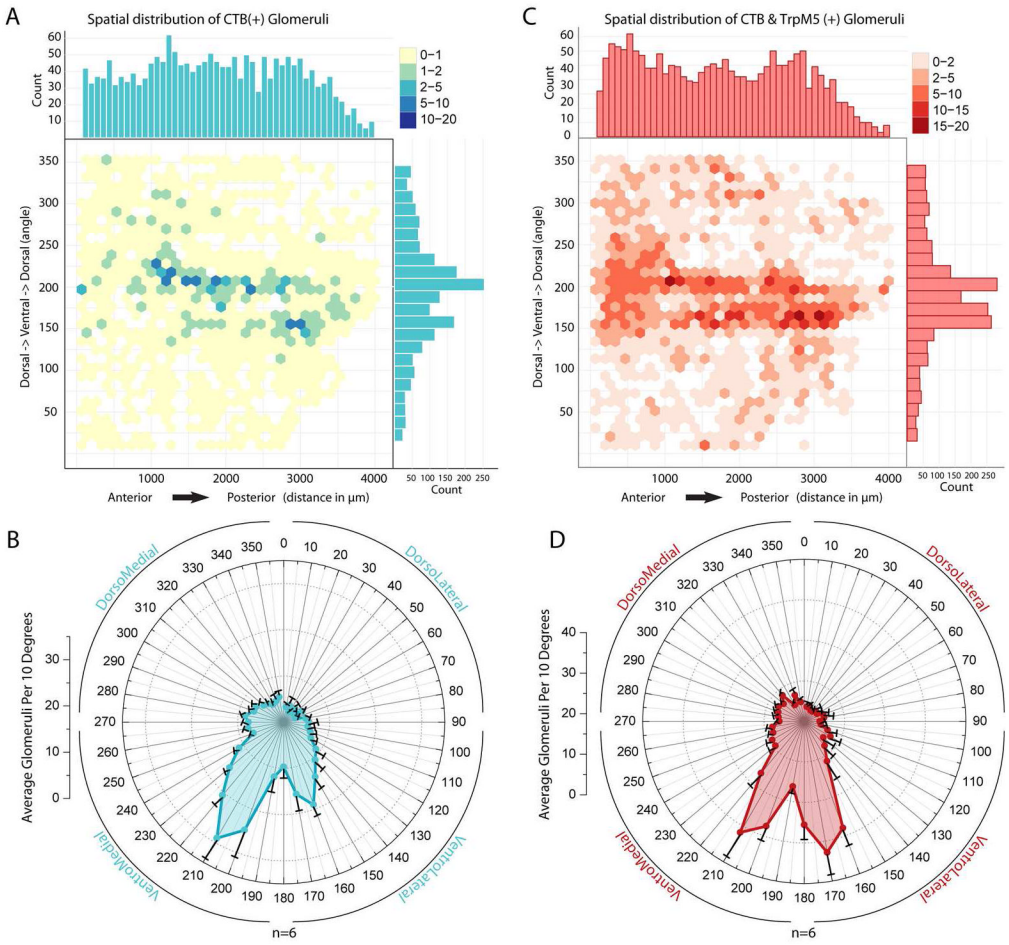

Figure 5.

CTB(+) and CTB(+) & TRPM5(+) glomeruli primarily observed in the ventral medial portion of the main olfactory. **A.** Spatial distribution and density of CTB(+) glomeruli for the dorsoventral and rostrocaudal axes across all cases. **B.** Distribution of CTB(+) glomeruli across the dorsoventral axis of the bulb for all cases with mean and SEM. **C.** Spatial distribution and density of CTB(+) & TRPM5(+) glomeruli for the dorsoventral and rostrocaudal axes across all cases. **D.** Distribution of CTB(+) & TRPM5(+) glomeruli across the dorsoventral axis for all cases with mean and SEM.

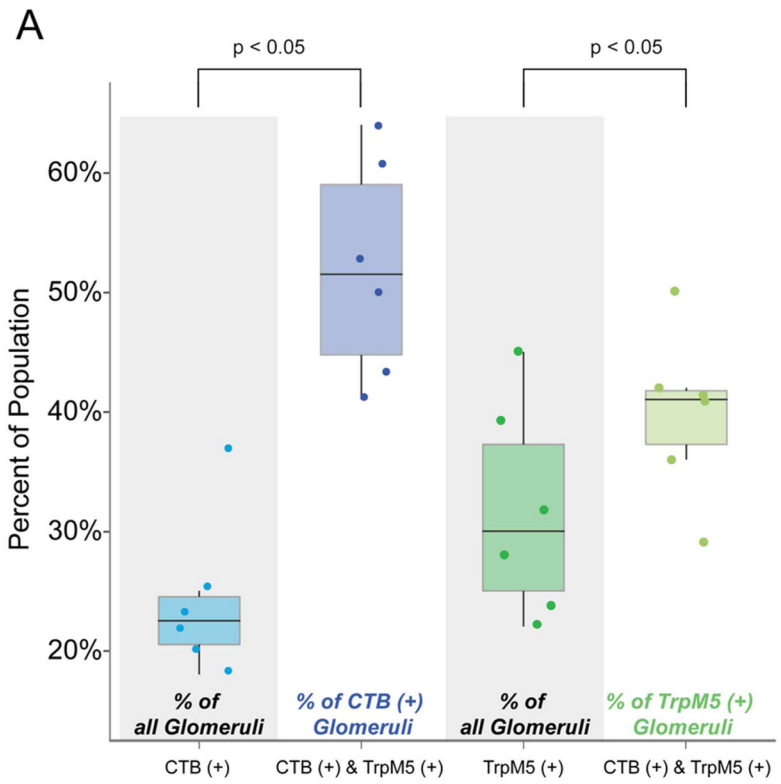

Figure 6.

Comparison of proportions of glomeruli showing CTB(+), TRPM5-GFP(+) and CTB(+) & TRPM5-GFP(+) colocalization. The four boxplots show the percent of the glomerular populations in six hemispheres. For each boxplot we show the median (the line in the middle of each box), the interquartile range (IQR; top and bottom of the box) and the whiskers (lines extending above and below each box indicate highest and lowest datum that falls within 1.5 x IQR). In addition, points show the percent of the population for each hemisphere. The percent of CTB(+) & TRPM5-GFP(+) colocalization within the CTB(+) and TRPM5-GFP(+) populations was significantly greater than the proportion of CTB(+) and TRPM5-GFP(+) glomeruli ($p < 0.05$ for both comparisons) in the total population indicating that the colocalization was likely greater than chance overlap.